

# Heat capacities (1 to 108 K) and linear thermal expansivities (1 to 300 K) of LuH<sub>0.148</sub> single crystals: Thermal relaxation effects and the pairing transition

C. A. Swenson

*Ames Laboratory and Department of Physics and Astronomy, Iowa State University, Ames, Iowa 50011*

(Received 30 November 1998)

Previous heat capacity ( $C_p$ ) and linear thermal expansivity ( $\alpha$ ) data for the hexagonal  $\alpha$ -LuH<sub>*x*</sub> and LuD<sub>*x*</sub> [LuH(D)<sub>*x*</sub>] single crystal alloys ( $x=0, 0.005, 0.053$ ) [C. A. Swenson, Phys. Rev. B **53**, 3680 (1996)] have been extended to LuH<sub>0.148</sub>. A feature (a transition) near 170 K in  $\alpha$  vs  $T$  for LuH<sub>0.053</sub> crystals is much more pronounced for the present results, with the  $c$ -axis ( $a$ -axis) data showing an almost 40% (30%) decrease (increase) in  $\alpha$  on cooling below 170 K. This transition, which was associated with the pairing of H along the  $c$  axis in next-nearest-neighbor tetrahedral sites on opposite sides of a lutetium ion, is not clearly defined, however, and, after a change in temperature, is characterized by isothermal drifts in the sample length with time constants which are very small at 175 K but increase to 100 h at 144 K. The migration energy associated with the temperature dependence of these time constants [0.26(3) eV] is approximately one-half that which is associated with high-temperature bulk diffusion. The conclusion is that pair breakup (pairing) does not occur (is not completed) at a unique transition temperature when the alloy is warmed (cooled), but is a thermally activated process, with the equilibrium fraction of paired H increasing with decreasing temperature, to achieve a saturation concentration below 140 K. The approach to pairing equilibrium for  $T < 175$  K is diffusion limited. [S0163-1829(99)04624-X]

## I. INTRODUCTION

The present data for the heat capacities ( $C_p$ ) and linear thermal expansivities ( $\alpha$ ) of  $a$ - and  $c$ -axis LuH<sub>0.148</sub> single crystals represent the extension of previous measurements on LuH<sub>*x*</sub> and LuD<sub>*x*</sub> [LuH(D)<sub>*x*</sub>] single crystals ( $x=0, 0.005, 0.053$ ) (Refs. 1 and 2) to a more concentrated alloy. The hexagonal  $\alpha$ -LuH(D)<sub>*x*</sub> alloys (together with similar alloys for yttrium and scandium) remain single phase to  $T=0$  for relatively large values of  $x$  ( $x < 0.25$ , or 20 at. %, for Lu).<sup>3,4</sup> At high temperatures, the hydrogens exist predominantly on the hcp tetrahedral ( $T$ ) sites in a random solid solution (the  $\alpha$  phase), but, on cooling, tend to align in pairs along the  $c$  axis in the next-nearest-neighbor (NNN)  $T$  sites on opposite sides of a rare-earth ion.<sup>5</sup> Resistivity annealing effects near 170 K (Refs. 4, 6) and rapid thermal-expansion changes near this temperature<sup>2</sup> have been associated with the cessation of pairing on cooling, or the onset of pair breakup on warming. This phenomenon has been referred to as the ‘pairing transition.’ This transition has appreciable width, and no clear dependence on  $x$  or on H isotope.<sup>2</sup>

Since pairing occurs along the  $c$  axis, thermal expansivity measurements on oriented single crystals provide a sensitive tool for studying the pairing transition on warming or cooling, above, below and within the transition. For  $x=0.053$ , the  $\alpha$  data showed small time-dependent length changes near 170 K which did not significantly affect the rather strong indications of the pairing transition.<sup>2</sup> Since the magnitude of the changes in  $\alpha$  near the transition was greater for LuH<sub>0.0053</sub> than for LuD<sub>0.0053</sub>, the present experiments involved only oriented single crystal LuH<sub>0.148</sub> alloys. The  $\alpha$  data for these samples show well-documented indications of nonequilibrium effects for data taken with both decreasing and increasing temperature for  $144 < T < 175$  K, or at temperatures

which are at or significantly below those normally associated with the pairing transition. The magnitudes of these effects were largest for  $c$ -axis LuH<sub>0.148</sub> and were studied in detail for this crystal, which also was the last to be measured. Data for the  $a$ -axis LuH<sub>0.148</sub> crystal are very similar to those for the  $c$  axis, but were not studied as extensively. The conclusion from these data, which will be documented in the following sections and figures, is that a pairing transition (that is, an  $x$ -dependent phenomenon at a fixed temperature) does not exist as such for LuH<sub>0.148</sub>. Rather, the equilibrium concentration of pairs appears to be a function of temperature which approaches saturation (100%?) at or below 140 K. The approach to equilibrium after a change in temperature is rapid for  $T \geq 175$  K, but is diffusion-limited at lower temperatures, and becomes extremely slow below 144 K, the lowest temperature for the present data.

The following section summarizes current evidence for the existence of pairing and a pairing transition in these alloys, and the temperature-dependence of the pair concentration. A brief description of the experimental apparatus and procedures will be followed by a presentation and discussion of the experimental data.

## II. LITERATURE SURVEY

This summary primarily includes information about the temperature-dependence of the paired fraction and time-dependent/diffusion-limited effects. The behavior of the scandium, yttrium, and lutetium H (D) alloys is qualitatively (and often quantitatively) very similar, and results for all three will be included. Daou and Bonnet<sup>4</sup> noted unusual low-temperature behavior in resistivity measurements on LuH(D)<sub>*x*</sub> alloys; these were intended, along with x-ray lattice parameter data, to study the limiting solubilities of H (D) in lutetium. The x-ray data include lattice parameters as a func-

tion of  $x$  at 25 °C, as well as  $a(T)$  and  $c(T)$  from room temperature to 550 °C for pure lutetium,  $\text{LuH}_{0.2}$  and  $\text{LuD}_{0.19}$ . A striking feature for these hexagonal metals is that the  $c/a$  ratio (which is larger for the alloys than for the pure metal; the  $c$  axis expands and the  $a$  axis contracts upon alloying) increases linearly with temperature from room temperature to 500 °C for the pure metal, but, for the alloys, becomes temperature-independent (the expansivities are isotropic) above approximately 250 °C after an initial linear increase with temperature.<sup>4</sup>

Subsequent isochronal resistivity studies used continuous heating (0.5 K/min) of  $\text{LuH(D)}_x$  (Refs. 6, 7) and similar rare-earth alloys<sup>8</sup> to investigate a resistivity annealing anomaly (a transition) near 170 K which occurred after quenching through this temperature or after low-temperature irradiation. They were able to establish binding energies associated with the transition [ $E_b = 0.05(1)$  eV], and also, from the isochronal annealing studies, a characteristic migration energy,  $E_m \approx 0.25$  eV. An analysis of these data gives a reaction of order unity.<sup>6</sup> An extensive summary of literature values for binding and migration energies for these alloys has been given by Vajda.<sup>9</sup> In a quite different experiment, Jung and Lässer<sup>10</sup> report the results of isothermal annealing measurements (160–180 K) of quenched resistivity samples of lutetium alloys with H, D, and T. The time scale for these data was a maximum of 2 h at 162 K. In contrast with the other resistivity studies, Jung and Lässer's data indicate (with considerable scatter) a reaction order  $\geq 2$ , and  $E_m = 0.45$  eV. More recently, Yamakawa and Maeta have measured isothermal resistivity recovery in quenched  $\text{LuH}_{0.12}$  samples.<sup>11</sup> The samples initially were quenched to liquid-nitrogen temperatures, then annealed at fixed temperatures of 140–162.5 K. The sample periodically was quenched in liquid nitrogen where the resistivity was determined; data taking extended over 5.5 days for the sample which was annealed at 140 K. These data are consistent with  $E_m = 0.43$  eV.

Nuclear magnetic resonance (NMR) also has been used to investigate these transitions.<sup>12</sup> The temperature dependences of the spin-lattice relaxation rates for  $\text{LuH}_{0.148}$  (Ref. 13),  $\text{YH}_{0.18}$  and  $\text{ScH}_{0.27}$  (Ref. 14) show structure near 180 K which indicates that the pairing transition involves a change in electronic structure.

Neutron-scattering experiments have been used to determine the temperature dependence of the structure [location, concentration, and distribution of the H (D) pairs] of these yttrium, scandium, and lutetium alloys. Inelastic neutron-scattering experiments show that the potential along the  $c$  axis at these NNN  $T$  sites is softer and more anharmonic than in the basal plane, so the predominant H (D) motion is along the  $c$  axis.<sup>15</sup> The small nearest-neighbor spacing for the tetrahedral sites does not allow pairs to be located on adjacent sites, and diffuse neutron-scattering data show that the pairs are ordered in an array of adjacent chains, with the chains possibly shorter for Sc than for Lu alloys.<sup>5</sup> A more recent inelastic-incoherent-neutron-scattering study suggests that the extent of ordering of these chains increases from  $\text{ScH}_x$  to  $\text{LuH}_x$  to  $\text{YH}_x$ .<sup>16</sup>

Although general agreement exists that the H (D) in Sc, Y, and Lu are paired across a metal ion and that the pairs exist in ordered  $c$ -axis chains, less conclusive evidence exists for the temperature at which pairs first appear on cooling,

and for the fraction of the H (D) which are paired as a function of temperature. Similarly, there is little evidence for the temperature at which the linear chain structure first appears, and for the growth of this structure on cooling. Diffuse neutron-scattering (DNS) experiments for  $\text{YD}_{0.17}$  (Ref. 17) relate the temperature dependence of the scattering structure factor to that of the pair density, and suggest that approximately 50% of the D were paired at 300 K, and 93% at 120 K. Similar results were obtained in other DNS experiments for  $\text{LuD}_x$  (Ref. 18) and  $\text{ScD}_x$  (Ref. 19). An analysis of temperature-dependent elastic incoherent neutron-scattering data for  $\text{YH}_{0.15}$  suggests that the number of pairs was essentially independent of temperature from 10 to roughly 170 K, after which it decreased by two-thirds upon heating to 390 K.<sup>20</sup> This analysis also verifies the  $c$ -axis H-Y-H pairing hypothesis by showing that the H-pair separation corresponds to the distance between NNN  $T$  sites in yttrium. The magnitude of the structure factor at a given temperature was associated with the number of unpaired H (D) which were jumping rapidly ( $10^{11} \text{ s}^{-1}$ ) between nearest-neighbor  $T$  sites ( $T$ - $T$  hopping), and, hence, reflected the breaking of pairs with increasing  $T$ . The unpaired (free) H (D) have been referred to as “labile,” while those which are paired (bound) are “nonlabile.”<sup>15</sup> This paper also presents results and further analyses of temperature-dependent structure factors associated with quasielastic-neutron-scattering (QENS) experiments on  $\text{YH(D)}_x$  (Ref. 21) and  $\text{ScH}_x$  (Ref. 22). In Refs. 15, 20, and 22, the temperature-dependent intensities and/or structure factors are normalized to low-temperature values, and should not be associated directly with complete pairing at low temperatures.

The detection of rapidly moving ( $T$ - $T$ ) protons as low as 10 K demonstrates that H (D) pairing probably is not complete at low temperatures.<sup>22</sup> A recent analysis<sup>23</sup> suggests that the QENS data for  $T > 150$  K and the lower temperature NMR experiments are measuring the same ( $T$ - $T$ ) proton motions, with hopping rates which increase rapidly with increasing temperature. The characteristic energy, 0.05 eV, is consistent with the H binding energy which is found in a number of quite different experiments.<sup>9</sup> At lower temperatures, the QENS hopping rates ( $> 10^{11} \text{ s}^{-1}$ ) increase with decreasing temperature, while the NMR rates decrease, resulting in QENS rates at 10 K which are approximately 1000 times greater than those observed in NMR measurements on the same materials.<sup>12</sup> This implies that QENS and NMR are looking at very different motions below 100 K, since the NMR motions are too slow for the QENS to see, while NMR cannot detect the much higher frequency QENS motions. Either a reasonable fraction of the H (D) remain unpaired below 100 K, or pairs are being broken and reformed continuously.<sup>23</sup>

A number of papers<sup>17,18,21,24</sup> attribute the 170 K resistivity transitions<sup>6</sup> to a freezing of the relaxation process. The bases for these suggestions arise from various measurements of H (D) diffusion in these alloys at relatively high temperatures. Hydrogen relaxation measurements gave the first determinations of H (D) diffusion in lutetium.<sup>25</sup> These were confirmed by Gorsky-effect measurements of the diffusion of H and D in single-crystal  $\text{LuH}_{0.05}$  and polycrystalline  $\text{LuH}_{0.05}$  and  $\text{LuD}_{0.05}$  from 380 to 540 K (Ref. 26) which showed that the diffusion is isotropic, with activation energies  $E_a$

$=0.575(15)$  eV for H and  $0.63(2)$  eV for D. These results are interpreted using a model in which hopping between nearest-neighbor  $T$  sites is very fast, and, because of the isotropy, diffusion in the basal plane is determined primarily by  $T$ - $O$ - $T$  jumps ( $O$  refers to octahedral sites). QENS measurements which were used to determine the occupancy times (jump rates) for the interstitial sites in polycrystalline  $\text{YH}_x$  (Ref. 27) and single crystal  $\text{YH}_{0.20}$  at 593, 633, and 695 K (Ref. 24) essentially agree with this model. The residence times for jumps between nearest neighbor  $T$  and  $O$  sites and from  $O$  to  $T$  sites are roughly comparable ( $10^{-10}$ – $10^{-11}$  s) at these temperatures, and are much smaller than those for jumps between  $T$  sites and  $O$  sites ( $10^{-9}$  s);<sup>24</sup> the resulting activation energy,  $E_a=0.57(3)$  eV, is in agreement with the Gorsky effect results.

An anelastic relaxation study of hydrogen pairs in  $\text{YH}_x$  single crystals<sup>28</sup> is consistent with other mechanical spectroscopy, high-temperature  $\text{ScH}_x$  NMR data<sup>29</sup> and neutron<sup>24,27</sup> results over 10 orders of magnitude in jump rates (a factor of almost 5 in  $T$ ), and an activation energy of  $0.60(3)$  eV. An extrapolation of these various results to 180 K gives a residence time of several minutes for the diffusion-limiting  $T$ - $O$  jump. Unfortunately, outside of a single observation of the doubling in 24 h of the intensity at 150 K of a  $\text{LuD}_{0.04}$  DNS scattering pattern,<sup>18</sup> there are no reports in the neutron-scattering literature of time-dependent effects.

The behavior of these alloys appears to be different at high and low concentrations,<sup>16,18,21</sup> with a decrease in chain order with decreasing  $x$ , and some question whether or not pair formation occurs for small  $x$ .<sup>21</sup> A small thermal expansivity pairing transition anomaly, however, exists for  $\text{LuH}_{0.005}$  and  $\text{LuD}_{0.005}$ .<sup>2</sup> A further analysis<sup>15</sup> of the data described in Ref. 21 shows that the temperature dependence of the elastic-incoherent-structure (EISF) is concentration-dependent for  $\text{YH}_x$ . This analysis of EISF data also includes more details of the data presented in Ref. 22. The model which is proposed for the EISF results links these data directly with the concentration of labile (free) H (D) in these alloys. A possibly related observation is that the temperature dependence of the low temperature  $C_p$  of  $\text{LuH(D)}_x$  shows a significant  $x$  dependence.<sup>2,30</sup> Below approximately 10 K,  $C_p(T)$  is qualitatively different for  $x \leq 0.015$  [where  $C_p(T)$  is anomalously large] and for  $x \geq 0.032$  [where  $C_p(T)$  is ‘‘normal,’’ see Ref. 2 for a discussion]. The absence of an isotope effect, and of a detectable similar contribution to the linear  $\alpha$ 's, rules out the association of the low- $x$   $C_p$  behavior with H (D) tunnelling. No explanation exists for this low-temperature  $C_p$  behavior; an association with the proposed the absence of pairing at low  $x$  is a possibility.

At higher temperatures, the  $C_p$  data for these  $\text{LuH(D)}_x$  alloys<sup>2</sup> are in agreement with phonon dispersion results which show small effects of pairing on the phonon spectrum.<sup>31</sup> The small  $x$  dependence of the alloy  $C_p$ 's (and  $\Theta_0$ 's) reflects the tight binding of a pair to its common Lu ion; the net effect of pairing on either side of a Lu ion is to increase slightly the mass of that ion. The pure lutetium  $C_p$ 's also agree well with those calculated from the phonon spectrum for pure lutetium.<sup>32</sup>

Cannelli *et al.*<sup>33</sup> have attributed a number of relaxation processes in measurements involving  $\text{YH}_x$  to interactions between hydrogen and oxygen in their samples. This possibility

generally does not arise in the work described above, since the original material for the samples (yttrium, scandium, lutetium) contained less than 0.01% oxygen.

### III. EXPERIMENTAL DETAILS

The sample preparation, experimental apparatus and procedures, data analysis, and, essentially, samples, were identical for the earlier<sup>2</sup> and the present measurements, so the relative  $C_p$  and  $\alpha$  data from these two investigations may be compared directly with better than  $\pm 1\%$  precision.  $H$  was added to the previous  $a$ - and  $c$ -axis  $\text{LuH}_{0.053}$  samples to obtain the current  $\text{LuH}_{0.148}$  samples.  $C_p$  data from 1 to 110 K were taken using a conventional semiadiabatic tray-type calorimeter with Apiezon- $N$  grease for thermal contact. The linear thermal expansivity data from 4 to 300 K were obtained using a copper differential capacitance dilatometer<sup>34</sup> which was calibrated using a copper standard.

Expansivity measurements are especially valuable for the study of systems which show hysteresis and time effects, since, in contrast with  $C_p$  experiments, data can be taken with either increasing or decreasing temperature. In addition, the extremely high (not always usable) sensitivity and stability ( $\delta L/L_{\text{sample}} \approx 2 \times 10^{-9}$  normally,  $2 \times 10^{-10}$  at low temperature) of this dilatometer make possible the determination of very small isothermal length instabilities.

### IV. RESULTS AND DISCUSSION

At low temperatures,  $C_p$  and  $\alpha$  for a pure metal are expected to follow the same temperature dependence, with<sup>1,35</sup>

$$C_p/T = \sum_{n=0}^N C_{2n+1} T^{2n} \quad (1a)$$

and

$$\alpha/T = \sum_{n=0}^N A_{2n+1} T^{2n}. \quad (1b)$$

These relations lead to the conventional  $C_p/T$  (or  $\alpha/T$ ) vs  $T^2$  plot of low-temperature data for metallic samples. The lead parameters ( $C_1$  and  $A_1$ ) generally arise from electronic contributions, while the  $C_3, A_3$  and higher-order parameters usually are associated with lattice contributions. For a pure metal,  $C_1 = \gamma$ , the electronic  $C_p$  coefficient, while the limiting lattice Debye temperature  $\Theta_0$ , can be calculated from  $C_3$  as

$$\Theta_0 = [1.944 \times 10^6 (\text{mJ/g mol K}) / C_3]^{1/3} \text{ K}. \quad (2)$$

If the  $C_p/T$  (or  $\alpha/T$ ) vs  $T^2$  representations of data show deviations from Eqs. (1) as  $T \rightarrow 0$  K, the implication is that an anomalous contribution to  $C_p(\alpha)$  exists. At higher temperatures, power series including all powers of  $T$  can be used more effectively to represent both  $C_p$  and  $\alpha$ , with the coefficients having no physical significance.<sup>1</sup> Power series fits to the data were used to generate the smooth representations of the data which appear as smooth curves in the following figures.

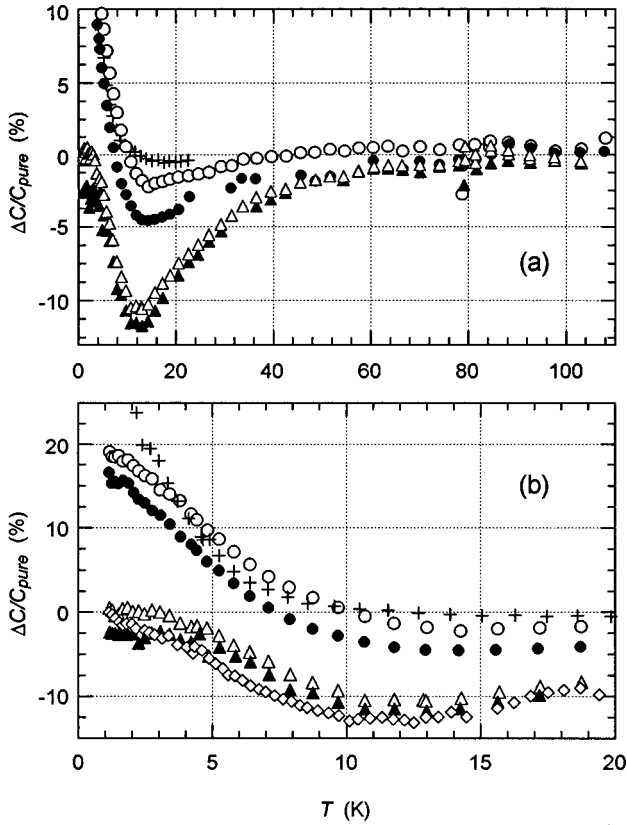


FIG. 1. The differences from the pure Lu  $C_p$  relation (Ref. 1) of the data for the individual samples of  $\text{LuH}_{0.148}$  [ $a$  axis ( $\Delta$ ),  $c$  axis ( $\blacktriangle$ )],  $\text{LuH}_{0.053}$  [ $a$  axis ( $\circ$ ),  $c$  axis ( $\bullet$ )] and  $c$ -axis  $\text{LuH}_{0.005}$  (+) (Ref. 2) and, in Fig. 1(b), polycrystalline  $\text{LuH}_{0.183}$  ( $\diamond$ ) (Ref. 30).

### A. $C_p$ results

The  $C_p$  data for the two  $\text{LuH}_{0.148}$  crystals are presented in Figs. 1 and 2, together with earlier results.<sup>1,2,30</sup> In Fig. 1(a), the differences of the various crystal data from the smooth relation for the pure initial material are systematic at low temperatures, but are less than  $\pm 1\%$  for  $T > 60$  K. Figure 1(b) shows the same  $C_p$ 's from 1 to 20 K with an expanded vertical axis, and also includes  $C_p$ 's for polycrystalline  $\text{LuH}_{0.183}$ .<sup>30</sup> The agreement between the data for the two  $\text{LuH}_{0.148}$  crystals and the polycrystalline data is quite satisfactory.

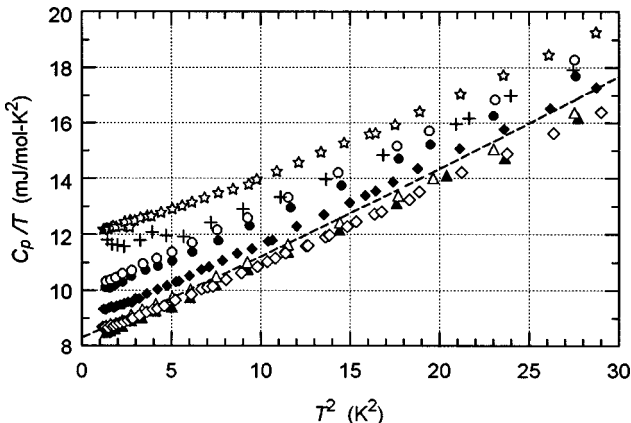


FIG. 2.  $C_p/T$  vs  $T^2$  for the crystal data [symbols as in Fig. 1, with pure Lu (— —)] and polycrystalline data [ $\text{LuH}_{0.015}$  ( $\star$ ),  $\text{LuH}_{0.124}$  ( $\blacklozenge$ ),  $\text{LuH}_{0.183}$  ( $\diamond$ )] (Ref. 30).

TABLE I. See Table I, Ref. 2. Parameters from fits to Eq. (1a) to the data in Fig. 2, and from the high-temperature normalizations of the  $\Theta/\Theta_0$  vs  $T/\Theta_0$  relation.  $\gamma$  is in units of  $\text{mJ/mol K}^2$ ,  $\Theta_0$  in K.

Sample alloy	Low $T$ fit		Normalized <sup>a</sup> $\Theta_0$	Citation
	$\gamma$	$\Theta_0$		
Initial crystal	8.299	189.9	189.9	Ref. 1
$c$ -axis $\text{LuD}_{0.053}$	9.770	189.1	192	Ref. 2
$c$ -axis $\text{LuH}_{0.053}$	9.715	193.8	193	Ref. 2
$a$ -axis $\text{LuH}_{0.053}$	9.939	189.0	191	Ref. 2
$a$ -axis $\text{LuH}_{0.148}$	8.300	188.1	195	Present
$c$ -axis $\text{LuH}_{0.148}$	8.072	189.3	195	Present
Pure Lu polycrystal	8.303	190.03	190.0	Ref. 30 <sup>b</sup>
Polycrystal $\text{LuH}_{0.032}$	10.776	194.9	192	Ref. 30 <sup>b</sup>
Polycrystal $\text{LuH}_{0.065}$	9.734	189.8	193	Ref. 30 <sup>b</sup>
Polycrystal $\text{LuH}_{0.124}$	8.886	192.9	196	Ref. 30 <sup>b</sup>
Polycrystal $\text{LuH}_{0.183}$	8.280	196.5	198	Ref. 30 <sup>b</sup>

<sup>a</sup>See Fig. 4, Ref. 2.

<sup>b</sup>See Ref. 2 for the data analysis which was used.

The lower temperature  $C_p$  data of Fig. 1(b), along with additional polycrystalline data,<sup>30</sup> are presented in the 1 to 5.5 K  $C_p/T$  vs  $T^2$  plot of Fig. 2. The purpose of this representation is to show that the data for pure lutetium,<sup>1</sup> single crystal  $\text{LuH}_{0.053}$  and  $\text{LuH}_{0.148}$ , and polycrystalline  $\text{LuH}_{0.124}$  and  $\text{LuH}_{0.183}$ , have approximately the same slope (with  $\Theta_0 = 190$  K). The primary differences arise through the  $T=0$  intercept  $\gamma$ , which decreases approximately linearly from  $10.8 \text{ mJ/mol K}^2$  at  $x=0.032$  (data<sup>30</sup> not shown) to the pure value near  $x=0.15$ . Columns 2 and 3 of Table I give the values of  $\gamma$  and  $\Theta_0$  from fits of Eq. (1a) to the various data for  $x \geq 0.032$ . For  $x < 0.032$ , the alloy data (the  $\text{LuH}_{0.015}$  and  $\text{LuH}_{0.005}$  data in Fig. 2 are typical) show anomalous behavior at low temperature. The polycrystalline  $\text{LuH}_{0.015}$  data represent the maximum observed difference of alloy  $C_p$ 's from those of pure lutetium for temperatures greater than 1 K.<sup>2,30</sup>

In Fig. 1, the  $\text{LuH}_{0.053}$  (and other) data show minima near 12 K which were ascribed in Ref. 2 to small changes in lattice properties; changes in  $\gamma$  of up to 25% were found to have negligible effects on  $C_p$  above 8 K because of the rapid increase of the lattice  $C_p$  with temperature. The shape of a lattice  $C_p(T)$  relation is reflected directly in the dimensionless  $\Theta(T)/\Theta_0$  vs  $T/\Theta_0$  relation, where  $\Theta(T)$  is an equivalent Debye temperature which is directly related to the lattice  $C_p(T)$ , and  $\Theta_0$  is an adjustable parameter characteristic of the lattice.<sup>2</sup> Using this formalism, the shapes of the lattice  $C_p$ 's for the various alloys (including now  $\text{LuH}_{0.148}$ ) can be made equivalent to those for pure lutetium using the values of  $\Theta_0$  in column 4 of Table I. The normalized  $\Theta_0$ 's vary approximately linearly with  $x$  (to within  $\pm 1$  K), with  $d \ln \Theta_0 / dx = 0.21(3)$ , in agreement with the earlier results and discussion.<sup>2</sup> There is no correlation with the large  $x$  dependence of  $\gamma$  which appears in column 2. The results in Table I suggest (but not clearly) that the normalized  $\Theta_0$ 's tend to be significantly larger than those obtained from the low-temperature fits of Eq. (1a) to the data. For lutetium, Eq. (1a) would be expected to give reliable values for  $\gamma$ , but small systematic errors in low-temperature  $C_p$  data can lead to significant uncertainties in  $\Theta_0$ .

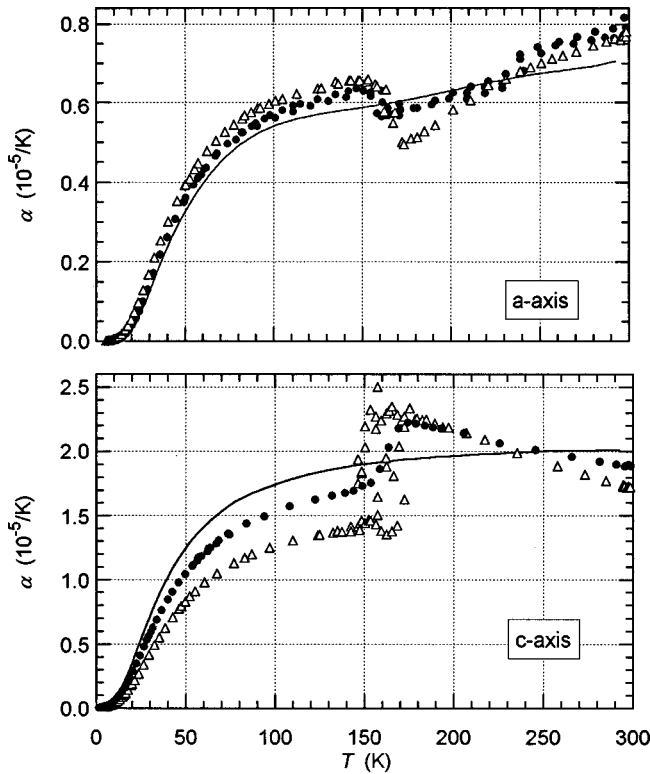


FIG. 3. *a*- and *c*-axis  $\alpha$  vs  $T$  data for the present  $\text{LuH}_{0.148}$  ( $\Delta$ ), pure Lu (—) (Ref. 1), and  $\text{LuH}_{0.053}$  ( $\bullet$ ) (Ref. 2). The *a*-axis vertical scale is more sensitive than that for the *c* axis.

The systematic differences between the  $C_p$ 's for the *a*- and *c*-axis  $\text{LuH}_{0.053}$  samples in Figs. 1 do not occur for  $\text{LuH}_{0.148}$ , even though the individual samples, except for H content, are the same. This introduces an added complication by suggesting that, as was previously noted,<sup>2</sup> subtle, unknown differences in sample preparation can be important for these alloys.

### B. Expansivity results

Figures 3 give the *a*- and *c*-axis linear thermal expansivity ( $\alpha$ ) data for the present  $\text{LuH}_{0.148}$  alloys, pure lutetium<sup>1</sup> and  $\text{LuH}_{0.053}$  (Ref. 2). Note the factor of 3 difference between the *c*-axis and *a*-axis  $\alpha$  scales, the opposite signs for the effects of alloying on the two crystal orientations, the relatively greater effects of alloying on the *c*-axis  $\alpha$ 's and, for  $x = 0.148$ , the qualitatively greater scatter of the data in the "transition region," 150–170 K. This scatter, which is related to drifts in sample length after a change in temperature, was studied in detail for the *c*-axis  $\text{LuH}_{0.148}$  sample, and less extensively, but with similar results, for the corresponding *a*-axis sample. The earlier *a*-axis  $\alpha$ 's,<sup>2</sup> in particular, showed significant scatter and hysteresis at all temperatures which are not understood.

Electronic contributions are important for pure lutetium  $C_p$ 's, but much more so for the  $\alpha$ 's, with the predominantly low-temperature electron-phonon and spin-fluctuation enhancements completely quenched by 100 K.<sup>1</sup> While  $C_p$  enhancements always must be positive, those for  $\alpha$  can have either sign, and are negative for the *a*-axis and positive for the *c*-axis  $\alpha$ 's.<sup>1</sup> Since these electronic contributions to  $\alpha$  (and

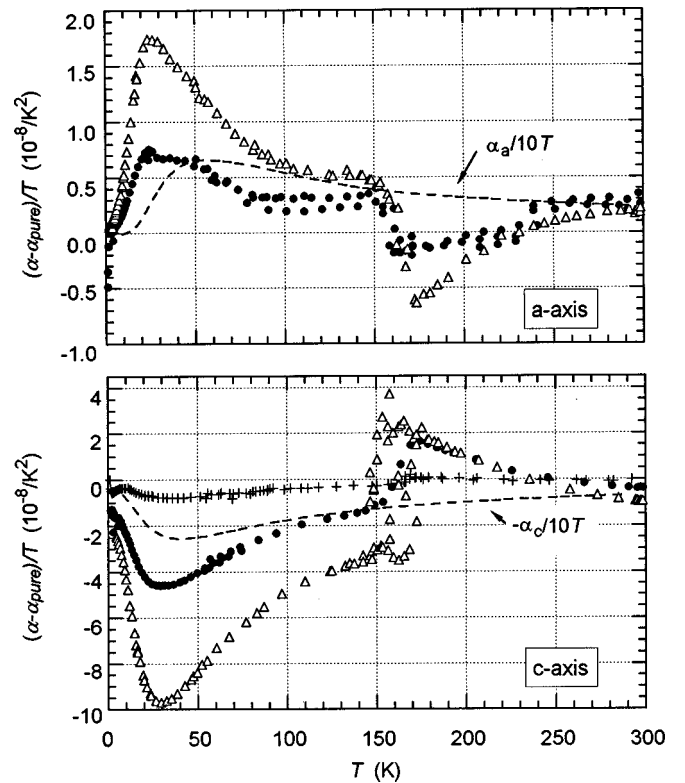


FIG. 4. Normalized *a*- and *c*-axis  $\alpha$ 's [ $(\alpha - \alpha_{\text{pure}})/T$  vs  $T$ ] for  $\text{LuH}_{0.148}$  ( $\Delta$ ),  $\text{LuH}_{0.053}$  ( $\bullet$ ), and *c*-axis  $\text{LuH}_{0.005}$  (+) (Ref. 2). The *a*-axis vertical scale is more sensitive than that for the *c* axis. For comparison, each figure includes  $\alpha/10T$  (---) for the pure crystal.

$C_p$ ) are expected to be proportional to temperature [Eq. (1b)], the differences between the alloy and pure metal properties also should, to a first approximation, be proportional to temperature. Figures 4 give the temperature dependence of the  $\alpha$  differences in Figs. 3 [ $\Delta\alpha = (\alpha - \alpha_{\text{pure}})$ ] after normalization by the temperature [ $\Delta\alpha/T$ ]. To establish a relative scale, each of Figs. 4 includes  $\alpha/10T$  (---) for the pure crystal. The steep decrease (increase) of  $\Delta\alpha/T$  with increasing temperature in the *c*-axis (*a*-axis) plots has been ascribed to a more rapid quenching of the enhancements in the alloys than for the pure metal.<sup>2</sup> While  $(\Delta\alpha/T)_{0\text{K}} = (\Delta\alpha/T)_{150\text{K}}$  for the *c*-axis alloys in Ref. 2 (indicating a change in the bare *c*-axis electronic properties on alloying), this does not apply to the *a*-axis data, nor to the *c*-axis  $\text{LuH}_{0.148}$   $\alpha$ 's in Figs. 4.

The low-temperature ( $<15\text{K}$ ) data in Figs. 3 and 4 are plotted as  $\alpha/T$  vs  $T^2$  in Figs. 5, where the *a*-axis and *c*-axis vertical scales differ by an order of magnitude. While these figures show that alloying has only a small effect on the *a*-axis  $A_1$  ("electronic") parameter, it has a large effect (almost linear in  $x$ ) for the corresponding *c*-axis term. This *c*-axis behavior is quite different from that of  $C_p$  in Fig. 2, where the  $T=0$  intercept ( $\gamma$ ) is not defined for  $x \leq 0.015$ , is abnormally large for  $x = 0.032$  and approaches the pure lutetium value for  $x > 0.15$ . In contrast with Fig. 2, the slopes ( $A_3$ ) in Fig. 5 have a strong  $x$  dependence (see the low- $T$  behavior in Figs. 4) which represent changes in electronic (an accelerated quenching of the enhancements), not lattice, properties.

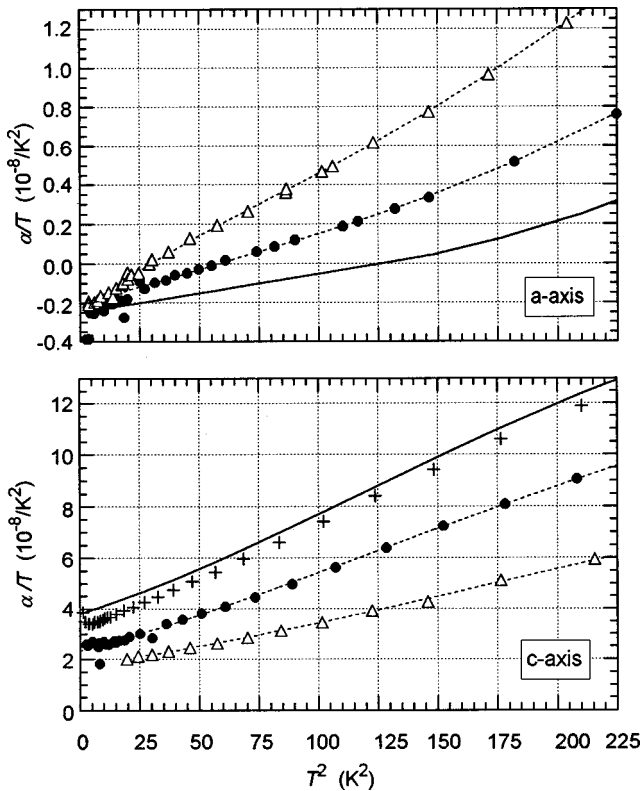


FIG. 5.  $\alpha/T$  vs  $T^2$  for the  $a$ - and  $c$ -axis data in Fig. 4. The dashed lines are fits of Eq. (1b) to the data. The  $a$ -axis vertical scale is an order of magnitude more sensitive than that for the  $c$  axis.

### C. The transition region; 144 to 170 K

Figure 6 shows details of the  $c$ -axis  $\text{LuH}_{0.148}$   $\alpha$  data from 110 to 210 K. Expansivity data were taken in three separate runs with the same setup [Run 1, 300–45–295 K; Run 2, (295)–4.2–55–(295) K; Run 3, (295)–175–144–175–(295) K], with only the first and last appearing in Fig. 6. For each data point, the dilatometer initially was in isothermal equilibrium at  $T$ , then was cooled (or warmed) to a new constant temperature,  $T + \Delta T$ ;  $\alpha$  was determined<sup>34</sup> from the changes

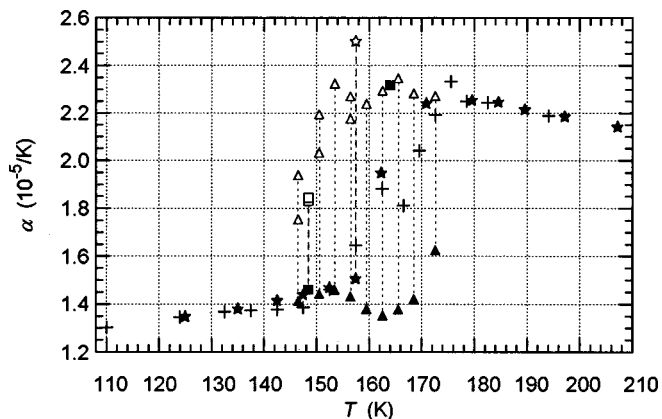


FIG. 6. Details from 110 to 210 K of the  $c$ -axis  $\text{LuH}_{0.148}$   $\alpha$ 's in Figs. 3 and 4. The dashed vertical lines connect  $\alpha$ 's calculated from data taken immediately after a temperature change (solid symbols) and those calculated after length drift was negligible (open symbols). Symbols; cool ( $\star$ ) and following warm ( $+$ ) for Run 1; cool ( $\blacktriangle$ ) and final warm ( $\blacksquare$ ) for Run 3. See the text for details.

in capacitance ( $\Delta C$ ), ( $\Delta T$ ), and  $\alpha(T)$  for copper.<sup>36</sup> The time constant for dilatometer equilibrium at 175 K is from 45 to 60 min, the temperature typically is constant to  $\pm 0.005$  K (5 mK) after 15 min or so [equilibrium control is  $\pm 1$  mK for several days], but thermal equilibrium (sample and cell isothermal, indicated by negligible capacitance drift) requires another 30 to 45 min. Typical  $\Delta T$ 's ranged from  $\pm 0.5$  K at liquid-helium temperatures to  $\pm 20$  K when  $\alpha$  had a small temperature dependence. For the data in Fig. 6,  $\Delta T$  usually was between ( $\pm$ ) 3 and 5 K. An important characteristic of the data for  $144 \leq T \leq 170$  K was a continuing isothermal drift in  $C$  after an hour or so, with a time constant appreciably larger than that for thermal equilibrium.  $C$ ,  $T$ , and  $dC/dt$  were recorded periodically until the drift rate was negligible.

The vertical dashed lines in Fig. 6 connect the  $\alpha$ 's calculated from the  $\Delta C$  immediately after temperature equilibrium was established (solid symbols) and the final  $\Delta C$  after the system showed negligible drift (open symbols). Where two open symbols are shown, the higher corresponds to an extrapolation of  $\Delta C$  to  $t = \infty$ . Data for Run 1 [on cooling from 300 to 45 K ( $\star$ ), then on warming back to 295 K ( $+$ )] were taken rather casually, before the significance of the drift was fully appreciated. These data were repeated in Run 3 (the same setup), with considerable care taken to document the effects of drift [cooling ( $\blacktriangle$ ), warming ( $\blacksquare$ )]. An important feature in Fig. 6 is that the solid symbols (neglecting drift) fall on an extrapolation to higher temperature of the  $T < 140$  K data (where time constants are very large), while the open symbols correspond to an extrapolation to lower temperatures of the  $T > 170$  K data, for which equilibrium is rapid.

Figures 7 give the capacitance [ $C(T, t)$ ] data which were used to calculate the  $\alpha$ 's in Fig. 6. The  $c$ -axis lutetium  $\alpha$ 's from 110 to 150 K fortuitously are only slightly larger than those for copper, with  $C$  varying slowly with temperature. A similar plot for the  $a$ -axis lutetium data (not shown) does not have the same clarity, primarily because both the  $\alpha$ 's and the relative effects in the transition region are smaller, and  $d\alpha/dT$  does not change sign at 160(10) K (Figs. 3).

The pattern for an  $\alpha$  determination in the transition region is as follows. In Fig. 7(b), the sample, initially in equilibrium (no drift) at 175 K ( $\blacktriangle$ ), is cooled to 170 K ( $\blacktriangle$ ), with the small  $\Delta C$  denoting an  $\alpha$  slightly greater than that for copper.  $C$ , however, drifts downwards isothermally (the gap,  $g$ , increases as the sample length shortens) towards equilibrium ( $\Delta$ ). The next cool, to 167 K, and subsequent cools, follow a step-wise path, and define two essentially parallel  $C(T)$  lines; the upper ( $\blacktriangle$ ), which corresponds to a nonequilibrium cooling (pair distribution "frozen"), and the lower ( $\Delta$ ), which presumably represents thermal equilibrium for the pairs and is an extrapolation of  $C(T)$  for  $T > 170$  K. After sample equilibrium at 144 K on the second run (lower  $\Delta$ ), the dilatometer was warmed to 153 K ( $\blacksquare$ ), with  $C$  subsequently increasing to an equilibrium value ( $\square$ ) which is on the lower of the two cooling lines; there is no hysteresis. An important observation in Fig. 7(b) is that the 144 K data do not lie on extrapolations of the linear relations. This corresponds in Fig. 6 to the decrease in the difference between the initial and the final  $\alpha$ 's below 150 K. Presumably, given sufficient time, pairing will be saturated just below 140 K.

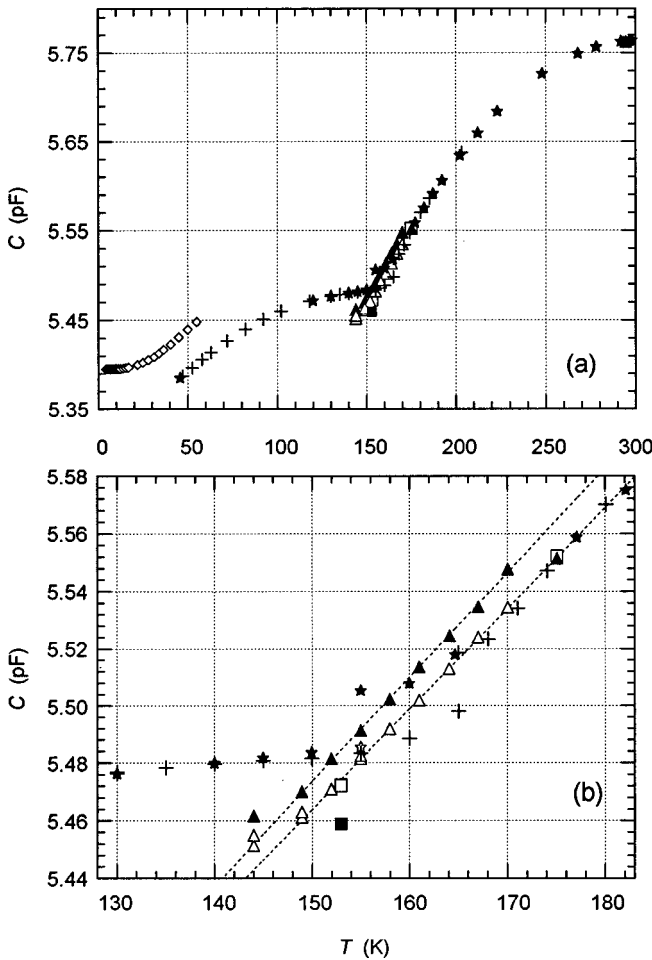


FIG. 7. Actual capacitance (relative length change) data vs  $T$  for the  $c$ -axis  $\text{LuH}_{0.148}$   $\alpha$ 's shown in Fig. 6. The symbols are as in Fig. 6, with the addition of 4 to 55 K data from Run 2 ( $\diamond$ ) in Fig. 7(a).

Figures 7 show apparent inconsistencies or shifts in the data near 50 K [Fig. 7(a)] and at 144 K. Figure 7(a) shows that data taken from 4 to 50 K in Run 2 (Figs. 3–5) immediately after Run 1 differ from Run 1 by  $+0.05$  pF ( $\delta L/L_s = +1.2 \times 10^{-4}$ ) near 50 K. For these low-temperature data, exchange gas was used to cool the dilatometer from 295 to 77 K over night without monitoring  $C(T)$ , after which the dilatometer was cooled to 4 K and data were taken to 55 K. The dilatometer subsequently was allowed to warm slowly back to 295 K; the initial and final 295 K  $C$ 's are in good agreement [indistinguishable in Fig. 7(a)]. Similarly, in Fig. 7(b), the 144 K  $C$ 's from Run 3 are 0.03 pF smaller than those from Run 1 (corresponding to  $\delta L/L_s = 7 \times 10^{-5}$ ) because the dilatometer was cooled through the transition region more quickly for Run 1 (+,  $\star$ ) than for Run 3 ( $\triangle$ ). A similar effect was observed for the  $a$ -axis  $\text{LuH}_{0.148}$  data ( $-0.015$  pF, same  $L_s$  and  $C$ 's) between the initial run (295–45–295 K) and a second run from 4 K upwards. The implication is that if a sample is cooled through the transition region too quickly,  $c$ -axis ( $a$ -axis) sample lengths below 100 K will be appreciably longer (shorter) than if a very slow, equilibrium, cooling rate had been used; a residual of unpaired H will remain. Unfortunately, these changes in sample length cannot be directly related to the number of pairs created.

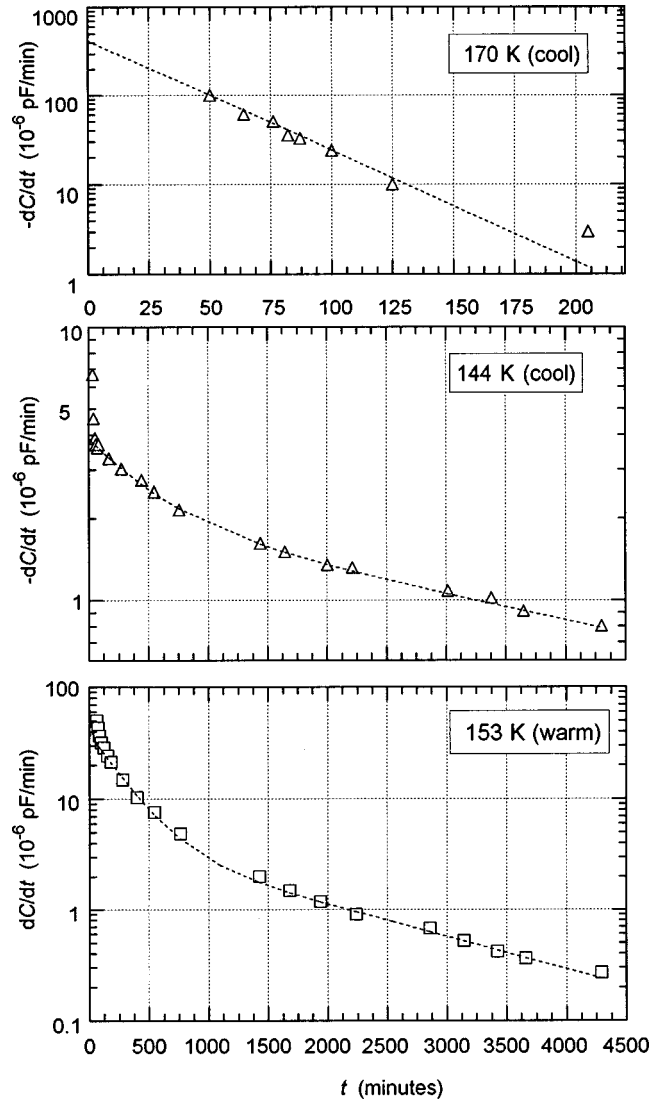


FIG. 8.  $dC/dt$  vs  $t$  for three of the Run 3 data points in Figs. 6 and 7. The symbols are as in those figures, with the dashed lines representing fits of Eq. (4) to these data; the time constants are shown in Fig. 9.

Figures 8 show isothermal  $dC/dt$  vs  $t$  relations for three of the Run 3 data in Fig. 7.  $dC/dt$ , which initially was  $-400 \times 10^{-6}$  pF/min ( $d \ln L_s/dt = -5.5 \times 10^{-5}/\text{h}$ ) at 170 K (cooling), was  $+0.15 \times 10^{-6}$  pF/min ( $d \ln L_s/dt = +2 \times 10^{-8}/\text{h}$ ) when the 153 K (warming) data were terminated. While the 170 K data showed negligible drift after 3.5 h, drifts for the 144 and 153 K data were appreciable after 3 days. Although the 170 K data in Fig. 8 can be represented by a single time constant  $\tau$ ,

$$[C(T, t) - C(T, t = \infty)] = [C(T, t = 0) - C(T, t = \infty)] \times \exp(-t/\tau) = \text{Pre} \times \tau \times \exp(-t/\tau), \quad (3a)$$

$$-dC/dt = \text{Pre} \times \exp(-t/\tau) = [C(T, t) - C(T, t = \infty)]/\tau, \quad (3b)$$

two time constants are required to represent the isothermal data in Figs. 6 and 7 below 165 K;

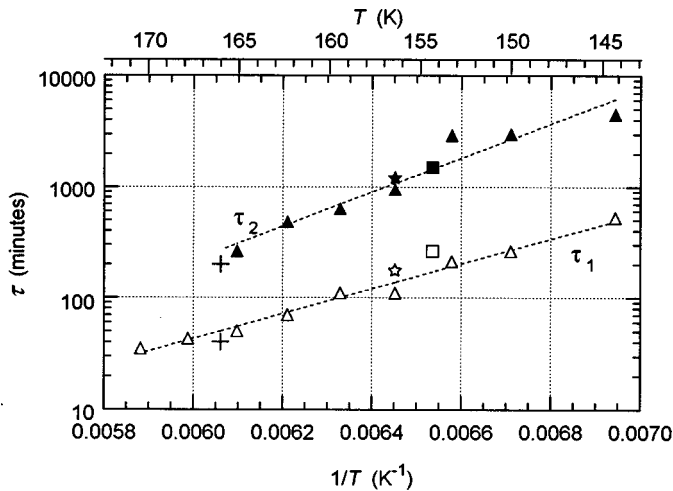


FIG. 9. Time constants  $\tau$  [Eq. (4)] vs  $1/T$  for the data in Figs. 6 and 7. The symbols are as in those figures.

$$dC/dt = \text{Pre1} \times \exp(-t/\tau_1) + \text{Pre2} \times \exp(-t/\tau_2). \quad (4)$$

The  $\tau$ 's for the data in Figs. 6–8 are plotted in Fig. 9 as  $\ln(\tau)$  vs  $1/T$ , the form which would be expected for a thermally activated process such as diffusion. The dashed lines represent least-squares fits to the  $\tau$ 's and give for the characteristic migration energies

$$E_{m1} = 0.22(1) \text{ eV and } E_{m2} = 0.31(4) \text{ eV.}$$

These are to be compared with the migration energies for H in lutetium from the isochronal resistivity recovery measurements, 0.27(2) eV,<sup>6</sup> from the isothermal resistivity recovery measurements, 0.45 eV (Ref. 10) and 0.43 eV (Ref. 11), and from the Gorsky effect determination of self-diffusion of H in lutetium, 0.575(15) eV.<sup>26</sup> The present average migration energy,  $(E_{m1} + E_{m2})/2 = 0.26(3)$  eV, agrees well with that from the isochronal resistivity measurements, which suggests that the two very different experiments are closely related. The differences from the two very difficult isothermal resistance recovery measurements (see Sec. II) is not understood. Similarly, it is not understood why the migration energies generally are appreciably smaller (50% smaller for the present data) than the bulk diffusion value. As was mentioned in Sec II, a number of papers have commented that an extrapolation of the bulk  $\text{LuH}_{0.05}$  diffusion results<sup>26</sup> gives occupation times of minutes near 180 K. These calculated occupation times, which are consistent with the onset of the present sample relaxations near 170 K, would be much shorter if the present migration energies were to be used. Hence, an inconsistency exists which is not understood.

For the present data, Eq. (3a) shows that the product  $\text{Pre} \times \tau \{ = [C(T, t=0) - C(T, t=\infty)] \}$  is proportional to the total isothermal (drift-related) change in length of the sample after a change in temperature. This relation can be used in two ways. First, Eq. (3b) can be used to estimate the difference between the capacitance at a time  $t$ ,  $C(T, t)$  and its limiting value  $C(T, t=\infty)$ , using  $dC(T)/dt$  at  $t$  and the appropriate  $\tau(t)$ ; for most of the data, the representation at the longest times was dominated by  $\tau_2$ . Second, if the total isothermal capacitance (length) change,  $\Delta C = [C(T, t=0) - C(T, t=\infty)]$ , is a measure of the equilibrium number of pairs

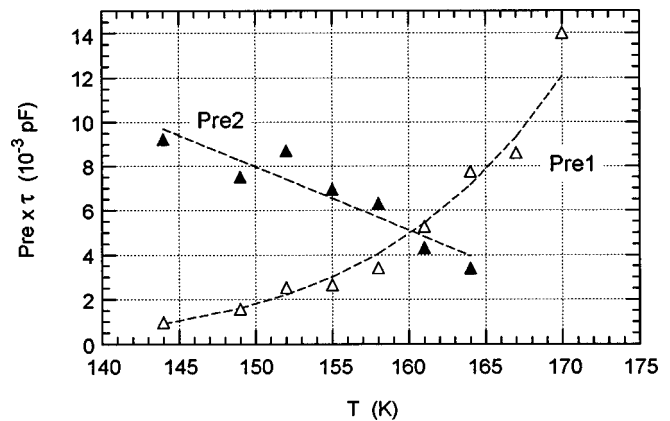


FIG. 10. The temperature dependence of the products  $\text{Pre} \times \tau$  for Pre1 and Pre2 from the fits of Eq. (4) to the data. The dashed line for Pre1 is from a fit of Eq. (5). See the text for details.

formed with changing temperature, the product  $\text{Pre} \times \tau$  should be, to first order, a thermally activated process, given by

$$\text{Pre} \times \tau = \text{const} \times \exp(-E/kT), \quad (5)$$

where  $E$  is a characteristic energy. Figure 10 is a plot of the products  $\text{Pre} \times \tau$  for Pre1 and Pre2. The dotted line through the Pre1 values represents a fit to Eq. (5) with  $E = 0.21(1)$  eV, in agreement with the characteristic energy associated with  $\tau_1$ . No similar analysis is applicable to the data for  $\text{Pre2} \times \tau_2$ , which has a very different temperature dependence, and for which an *ad hoc* linear relation has been plotted.

The representation of the  $dC/dt$  vs  $t$  data with two time constants [Eq. (4)] is not unique, but was used for convenience, and involves the implicit assumption that the pairing reaction is of order unity. This assumption is suspect, since H must occupy the  $T$  sites simultaneously in order for the reaction (pair formation) to occur. An isothermal resistivity recovery study which is more analogous to the present work, gave a reaction order of 2 or more, with  $E_m = 0.45$  eV (Ref. 10). An attempt was made to apply the formalism from this study<sup>10</sup> to the 144 K data in Fig. 8, with no success. Independent of the choice of a reaction order, the data always showed a change in character approximately midway through. The analysis of the most recent isothermal resistivity recovery studies<sup>11</sup> states that the results are independent of the assumption of a reaction order.

The discussion of the x-ray-diffraction measurements<sup>4</sup> in Sec. II noted the different temperature dependences of the  $c/a$  ratios of pure Lu and  $\text{LuH}_x$ . The pure lutetium expansivities<sup>1</sup> and those for  $\text{LuH}_{0.148}$  can be used to calculate the  $c/a$  relations for  $T < 300$  K which are shown in Fig. 11; the  $\alpha$ 's were integrated to obtain relative  $a$ - and  $c$ -axis length changes which were normalized to the  $c$  and  $a$  x-ray values at 300 K.<sup>4</sup> The linear temperature dependence of  $c/a$  for the pure metal, and the concave downwards temperature dependence for  $\text{LuH}_{0.148}$  above 170 K are consistent with the higher temperature x-ray data.<sup>4</sup> For the alloy, an extrapolation of the low-temperature curve to higher temperatures and of the higher temperature curve to lower temperatures suggests that the change in character occurs near 150 K; this



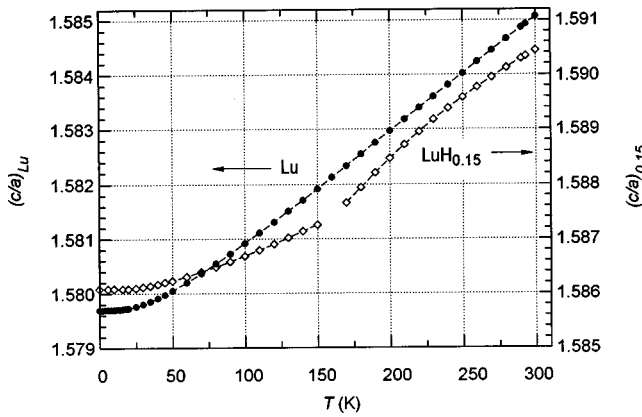


FIG. 11.  $c/a$  vs  $T$  for pure lutetium ( $\bullet$ ) and for  $\text{LuH}_{0.148}$  ( $\diamond$ ) as calculated from an integration of the smooth single crystal  $\alpha$ 's. Note the offset in the scales for the two materials.

does not rule out a transition, but is consistent with the interpretation of the present data. Higher temperature data would be interesting to, possibly, relate the temperature variation of  $c/a$  to the onset and temperature dependence of the formation of pairs.

## V. CONCLUSIONS

The initial objective of the present investigations was to extend previous  $\alpha$  and  $C_p$  data for single crystal  $\text{LuH}_x$  alloys<sup>2</sup> from  $x=0.053$  to  $x=0.148$ . The general trends exhibited by the earlier data are confirmed, with the  $C_p$  results below 20 K in agreement with polycrystalline data.<sup>30</sup> The large differences between the shapes of the pure metal and alloy  $\alpha$ 's in Ref. 2 are enhanced (but do not scale with  $x$ ) for  $\text{LuH}_{0.148}$  (Figs. 3 and 4).

In Figs. 3, the abrupt change in  $\alpha$  below 170 K occurs near the same temperatures where relaxation effects (often referred to as the pairing transition) initially were observed in resistance recovery studies of the annealing of quenched and/or irradiated samples.<sup>6</sup> These effects generally were associated with the lowest temperature at which, on cooling, H pairs are formed along the  $c$  axis in the NNN  $T$  sites on either side of a Lu ion. A number of papers<sup>17,18,21,24</sup> suggest, however, that this apparent transition is the result of the slowing down of H diffusion in these alloys, and, on the basis of high-temperature bulk diffusion measurements,<sup>26</sup> predict a dwell time of the order of minutes near 180 K. In Figs. 3 and 4, the scatter of the  $\text{LuH}_{0.148}$   $\alpha$  data below 175 K is related directly to long-term drifts in sample length after a change in temperature; these effects are documented in Fig. 6, where the solid symbols ( $\blacktriangle$ ) are for data taken immediately after a change in temperature, while the open symbols ( $\triangle$ ) are for data taken after the drifts have become negligible. When  $\alpha$  in this transition region is determined by cooling the sample, the initial  $\alpha$ 's reflect a decrease in sample length with a "frozen" pair distribution. As additional pairs begin to form, the sample length decreases (pair formation causes the lattice parameters  $c$  to decrease and  $a$  to increase) until an equilibrium is reached; the  $\alpha$  calculated from the equilibrium state is larger than that from the state immediately after the temperature change. The implications from these data are that the equilibrium relative number of pairs is a smooth function

of temperature, and that a pairing transition as such does not exist. For extremely slow changes in temperature, the paired fraction appears to saturate near or below 140 K. Figures 7 show the raw capacitance data which were used to calculate the  $\alpha$ 's in Fig. 6. The systematic capacitance differences between the three runs [near 50 K in Fig. 7(a), at 144 K in Fig. 7(b)] are a direct consequence of the rate of cooling of the sample; a larger  $C$  is associated with a more rapid cooling rate through the transition region and implies a greater sample length and fewer pairs formed. Unfortunately, no direct correlation exists between isothermal changes in sample length and the number of pairs created.

The isothermal resistivity recovery measurements of Jung and Lässer<sup>10</sup> (160–180 K) and Yamakawa and Maeta<sup>11</sup> (140–163 K) qualitatively support this picture, and extend the lowest temperature to 140 K. Their data show that the rate of resistance recovery after quenching slows dramatically as the temperature is decreased, with time scales which are comparable with the present.

Fast H motion between NN  $T$  sites has been observed below 100 K in neutron-scattering experiments.<sup>22</sup> This observation has been used to postulate that nonpaired ("labile") H exist at low temperature's. Other experiments<sup>15,17–21</sup> also give information about paired fractions as a function of temperature. The present experiments indicate that pair formation most likely does not take place, or occurs infinitely slowly, below 140 K [(very) slow cooling rates are essential for pairing equilibrium], and imply that, for "rapid cooling," a significant unpaired fraction could exist. The only mention in the neutron-scattering literature of time-dependent effects is a single observation of the doubling in 24 h of the intensity at 150 K of a  $\text{LuD}_{0.04}$  DNS scattering pattern.<sup>18</sup> The time scales in the transition region for the isochronal resistivity recovery experiments,<sup>6</sup> which are measured in minutes, are much shorter than those for the present experiments, which range from hours to days. These differing time scales may account for some of the differences in the conclusions.

A representation of the time-dependence of the  $c$ -axis drift rates for  $T < 167$  K (Fig. 8) requires the use of two time constants [Eq. (4), Fig. 9]. The average of the migration energies for the two time constants, 0.26(3) eV, is the same as that determined in the isochronal resistivity recovery experiments,<sup>6</sup> 0.27(2) eV, which suggests that the two quite different experiments involve the same phenomenon. A puzzling discrepancy is that the magnitude of this migration energy is just one-half of that for self-diffusion,<sup>25,26</sup> 0.575(15) eV. The two isothermal resistance recovery experiments give  $E_m = 0.45$  eV (Ref. 10) and 0.43 eV (Ref. 11), with no uncertainties stated. Each of the resistance recovery experiments involves at least one crucial assumption. The experimental data of Daou *et al.*<sup>6</sup> are consistent with a reaction order of 1, while those of Jung and Lässer<sup>10</sup> suggest a reaction order of 2 or greater. Yamakawa and Maeta<sup>11</sup> state that their results are independent of the assumption of a reaction order, but (implicitly) assume that the shape of the resistance-temperature relation is independent of pair concentration. While the present isothermal experiments have much greater precision than any of the resistivity experiments, and, hence, should be more reliable, a unique interpretation is not possible since the data below 167 K cannot be represented by a single time constant, nor by the assump-

tion of a reaction order greater than unity. A puzzling semi-qualitative feature common to all of these experiments is that the migration energy for each is significantly smaller than that for high-temperature bulk diffusion, yet the larger bulk diffusion value is consistent with the onset of diffusion-limited recovery effects near 180 K.

The temperature dependence of the product of the pre-exponential term and the corresponding time constant reflects the magnitudes of the total capacitance (length) changes which will occur during these isothermal drifts. Figure 10 shows these products for the two time constants. The behavior of  $\text{Pre1} \times \tau_1$  can be interpreted to be proportional to the increase in the unpaired H population with increasing temperature; the dotted line [Eq. (5)] assumes a thermally activated process with the same activation energy for  $\tau_1$  (0.22 eV) as in Fig. 9. This is an interesting, and perhaps significant, coincidence. As an unsubstantiated conjecture, the product  $\text{Pre2} \times \tau_2$ , which increases with decreasing temperature, could be associated with the formation of paired H chains.<sup>5</sup>

The  $C_p(T)$  results of Thome *et al.*<sup>30</sup> for polycrystalline  $\text{LuH}_x$  show that a qualitative difference in character occurs for  $0.015 < x < 0.032$ , with a maximum deviation from those for pure lutetium for  $x$  in this interval. In Fig. 2, the  $c$ -axis  $\text{LuH}_{0.005}$  (+) and the polycrystalline  $\text{LuH}_{0.015}$  (☆) data have a pronounced upturn as temperature approaches zero, while the higher  $x$  (and pure lutetium) data behave “normally” [Eq. (1a)], with approximately the same lattice contribution. In addition, for  $x \geq 0.032$ , the electronic  $C_p$  coefficients,  $\gamma$  (Table I), decrease almost linearly with increasing  $x$  (by 30%) to the pure value near  $x = 0.15$ . No explanations exist for these behaviors; the lack of an isotope effect has ruled out tunneling as a mechanism for the small  $x$  anomalies.<sup>2</sup> A possible correlation with the neutron results arises through the observation that alloy behavior is different for low and

high concentrations,<sup>15,16,18,21,22</sup> with a question as to whether pairing even occurs for small  $x$ ,<sup>21</sup> although a pairing transition occurs for  $x = 0.005$  in the  $\alpha(T)$  data.<sup>2</sup> An interesting experiment would be to compare low-temperature  $C_p$  data for a sample which, initially, was cooled rapidly through the transition region and then very slowly. No cooling rate-dependent data exist for the current  $C_p$  experiments;<sup>2,30</sup> the time spent in the transition region probably was less than 1 h. Additional  $C_p$  data for  $0.015 \leq x \leq 0.032$  also would be useful. The previous suggestion<sup>2</sup> that  $C_p$  measurements in the transition region would be helpful probably no longer applies, since the temperature-dependent relaxation times would make the interpretation of  $C_p$  data difficult. The data from the single report of  $C_p$  data for the transition region<sup>7</sup> are inconclusive.

The early x-ray investigations of Daou *et al.*<sup>4</sup> suggest that an extension of the single crystal length-change data to 500 °C or so, probably by using x-ray or neutron-diffraction techniques, would be extremely useful. In particular, the temperature dependence of the lattice parameters or the  $c/a$  ratio (Fig. 11) could provide clues as to the onset of pairing in an alloy such as the present.

#### ACKNOWLEDGMENTS

The detailed investigation of time effects in these alloys was suggested by Dr. Richard G. Barnes, who has been extremely helpful in proving much background information and advice. Very useful correspondence with Dr. Peter Vajda also is acknowledged. The  $\text{LuH}_{0.148}$  samples were prepared and characterized by Dr. David T. Peterson at the Materials Preparation Center of the Ames Laboratory. This work was performed at the Ames Laboratory, Iowa State University and was supported by the Director of Energy Research, Office of Basic Science, U.S. Department of Energy under Contract No. W-7405-ENG-82.

<sup>1</sup>C. A. Swenson, Phys. Rev. B **53**, 3669 (1996).

<sup>2</sup>C. A. Swenson, Phys. Rev. B **53**, 3680 (1996).

<sup>3</sup>B. J. Beaudry and F. H. Spedding, Metall. Trans. B **6B**, 419 (1975).

<sup>4</sup>J. N. Daou and J. E. Bonnet, J. Phys. Chem. Solids **35**, 59 (1974).

<sup>5</sup>O. Blaschko, J. Less-Common Met. **172-174**, 237 (1991).

<sup>6</sup>J. N. Daou, P. Vajda, A. Lucasson, P. Lucasson, and J. P. Burger, Philos. Mag. A **53**, 611 (1986).

<sup>7</sup>P. Vajda, J. N. Daou, J. P. Burger, K. Kai, K. A. Gschneidner, Jr., and B. J. Beaudry, Phys. Rev. B **34**, 5154 (1986).

<sup>8</sup>J. P. Burger, J. N. Daou, A. Lucasson, P. Lucasson, and P. Vajda, Z. Phys. Chem., Neue Folge **143**, 111 (1985).

<sup>9</sup>P. Vajda, in *Handbook on the Physics and Chemistry of the Rare Earths*, edited by K. A. Gschneidner, Jr. and L. Eyring, Vol. 20 (North-Holland, New York, 1995), p. 232.

<sup>10</sup>P. Jung and R. Lässer, J. Alloys Compd. **190**, 25 (1992).

<sup>11</sup>K. Yamakawa and H. Maeta, J. Alloys Compd. **248**, 77 (1997).

<sup>12</sup>Richard Barnes, J. Less-Common Met. **172-174**, 509 (1991).

<sup>13</sup>D. R. Torgeson, J.-W. Han, C.-T. Chang, L. R. Lichty, R. G. Barnes, E. F. W. Seymour, and T. W. West, Z. Phys. Chem., Neue Folge **164**, 853 (1989).

<sup>14</sup>L. R. Lichty, J.-W. Han, R. Ibanez-Meier, D. R. Torgeson, R. G.

Barnes, E. F. W. Seymour, and C. A. Sholl, Phys. Rev. B **39**, 2012 (1989).

<sup>15</sup>N. F. Berk, J. J. Rush, T. J. Udovic, and I. S. Anderson, J. Less-Common Met. **172-174**, 496 (1991).

<sup>16</sup>T. J. Udovic, J. J. Rush, I. S. Anderson, J. N. Daou, P. Vajda, and O. Blascho, Phys. Rev. B **50**, 3696 (1994).

<sup>17</sup>M. W. McKergow, D. K. Ross, J. E. Bonnet, I. S. Anderson, and O. Schaerpf, J. Phys. C **20**, 1909 (1987).

<sup>18</sup>O. Blaschko, G. Krexner, J. Pleschiutchnig, G. Ernst, J. N. Daou, and P. Vajda, Phys. Rev. B **39**, 5605 (1989).

<sup>19</sup>O. Blaschko, J. Pleschiutchnig, P. Vajda, J. P. Burger, and J. N. Daou, Phys. Rev. B **40**, 5344 (1989).

<sup>20</sup>J. E. Bonnet, D. K. Ross, D. A. Faux, and I. S. Anderson, J. Less-Common Met. **129**, 287 (1987).

<sup>21</sup>I. S. Anderson, N. F. Berk, J. J. Rush, and T. J. Udovic, Phys. Rev. B **37**, 4358 (1988).

<sup>22</sup>I. S. Anderson, N. F. Berk, J. J. Rush, T. J. Udovic, R. G. Barnes, A. Magerl, and D. Richter, Phys. Rev. Lett. **65**, 1439 (1990).

<sup>23</sup>R. G. Barnes (private communication).

<sup>24</sup>I. S. Anderson, D. K. Ross, and J. E. Bonnet, Z. Phys. Chem., Neue Folge **164**, 923 (1989).

<sup>25</sup>P. Vajda, J. N. Daou, and P. Moser, J. Phys. (France) **44**, 543 (1983).

- <sup>26</sup>J. Völkl, H. Wipf, B. J. Beaudry, and K. A. Gschneidner, Jr., *Phys. Status Solidi B* **144**, 315 (1987).
- <sup>27</sup>I. S. Anderson, A. Heidemann, J. E. Bonnet, D. K. Ross, S. K. P. Wilson, and M. W. McKergow, *J. Less-Common Met.* **101**, 405 (1984).
- <sup>28</sup>B. Kapesser, H. Wipf, R. G. Barnes, and B. J. Beaudry, *Europhys. Lett.* **36**, 385 (1996).
- <sup>29</sup>J-W. Han, C-T. Chang, D. R. Torgeson, E. F. W. Seymour, and R. G. Barnes, *Phys. Rev. B* **36**, 615 (1987).
- <sup>30</sup>D. K. Thome, K. A. Gschneidner, Jr., G. S. Mowry, and J. F. Smith, *Solid State Commun.* **25**, 297 (1978).
- <sup>31</sup>O. Blaschko, G. Krexner, L. Pintschovius, P. Vajda, and J. N. Daou, *Phys. Rev. B* **38**, 9612 (1988).
- <sup>32</sup>J. Pleschiutchnig, O. Blaschko, and W. Reichardt, *Phys. Rev. B* **41**, 975 (1990).
- <sup>33</sup>G. Cannelli, R. Cantelli, F. Cordero, F. Trequattrini, and A. Sermoneta, *J. Alloys Compd.* **253-254**, 367 (1997).
- <sup>34</sup>C. A. Swenson, in *Thermal Expansion of Solids*, edited by C. Y. Ho and R. E. Taylor, CINDAS Data Series on Material Properties, Vol. 1-4 (ASM International, Materials Park, OH, 1998), Chap. 8, p. 219.
- <sup>35</sup>T. H. K. Barron, J. G. Collins, and G. K. White, *Adv. Phys.* **29**, 609 (1980).
- <sup>36</sup>F. R. Kroeger and C. A. Swenson, *J. Appl. Phys.* **48**, 853 (1977).